Available online at www.sciencedirect.com
SCIENCE DIRECT®
Journal of Catalysis 225 (2004) 259–266
JOURNAL OF CATALYSIS
www.elsevier.com/locate/jcat

Preferential oxidation of carbon monoxide in the presence of hydrogen (PROX) over ceria–zirconia and alumina-supported Pt catalysts

Attila Wootsch,[a,b,*] Claude Descorme,[a,c] and Daniel Duprez [a]

[a] *LACCO-UMR 6503, CNRS-Université de Poitiers, 40, Avenue du Recteur Pineau, F-86022 Poitiers cedex, France*
[b] *Institute of Isotope and Surface Chemistry, CRC, HAS, Budapest PO Box 77, H-1525, Hungary*
[c] *Institut de Recherches sur la Catalyse (IRC), CNRS, 2, Avenue Albert Einstein, F-69626 Villeurbanne cedex, France*

Received 11 December 2003; revised 16 March 2004; accepted 15 April 2004

Abstract

One crucial requirement for the operation of proton exchange membrane fuel cells (PEMFC) is to feed carbon monoxide free hydrogen to the anode. This need can be achieved by using catalysts able to selectively oxidize CO in the presence of excess hydrogen. Herein we report the preferential CO oxidation (PROX) in the presence of hydrogen over $Pt/Ce_xZr_{x-1}O_2$ ($x = 0$, 0.15, 0.5, 0.68, 1) catalysts. A comparison with results observed on a Pt/Al_2O_3 catalyst is also presented. We examined the effect of temperature (90–300 °C) and O_2 excess ($\lambda = 0.8$–2). Ceria-supported platinum catalysts were more active than Pt/Al_2O_3 in both CO and H_2 oxidation. The result was a sharp "light off" around 90 °C for the oxygen conversion. The maxima, which appeared in the CO conversion and in the selectivity toward CO oxidation as a function of temperature on Pt/Al_2O_3, did not show up in the case of ceria-supported samples. Chloride ion-containing Pt/CeO_2 catalysts showed lower performances in the PROX reaction, especially at low temperatures. Four types of reaction mechanisms were suggested for $Pt/Ce_xZr_{x-1}O_2$ samples: (i) competitive Langmuir–Hinshelwood CO and hydrogen oxidation on Pt particles, (ii) noncompetitive Langmuir–Hinshelwood mechanism on the metal/oxide interface, (iii) hydrogen oxidation on the support, and (iv) water–gas-shift reaction at high temperatures. The second reaction route predominated at low temperatures (90–130 °C) and was found preferential to CO oxidation rather than hydrogen–oxygen reaction. This process was selectively blocked by Cl ions. The possible application of Pt/CeO_2 and Pt/Al_2O_3 catalysts was discussed. Ceria appeared as a suitable support for the preferential CO oxidation catalysts at low temperatures.

Keywords: Preferential CO oxidation; PROX; Platinum; Pt/CeO_2; Ceria; Ceria–zirconia; Oxygen mobility; Hydrogen purification; Fuel cell

1. Introduction

Application of fuel cell-powered systems to transportation recently has received increasing attention because of their theoretical high fuel efficiency and low environmental impact [1,2]. Numerous types of fuel cells have already been developed [1,2]. Among them, one of the most promising is the proton exchange membrane fuel cell (PEMFC) fueled with hydrogen [1–3]. However, depending on the type of anode, the CO concentration in the hydrogen feed must be under 1–100 ppm [1,4]. Hydrogen is usually produced by steam reforming (STR), autothermal reforming (ATR), or partial oxidation (POX) of natural gas, light oil fractions, and alcohols [5–7]. Unfortunately, a noticeable amount of CO, ca. 5–15%, is formed together with H_2, H_2O, and CO_2. A subsequent water–gas-shift (WGS) stage reduces the amount of CO to 0.5–1% [4–6]. This high amount of CO can be removed by *pr*eferential *ox*idation (PROX) and/or by methanation of CO using mainly Pt and Pt–Ru bimetallic catalysts [8,9].

Oh and Sinkevitch published the first general work on the PROX in 1993 [10]. They tested a variety of noble metals, such as Ru, Rh, Pt, and Pd on alumina support as well as other possible oxidation catalysts, such as Co/Cu, Ni/Co/Fe, Ag, Cr, Fe, and Mn, respectively. Platinum, rhodium, and ruthenium were found to be the most appropriate for the PROX reaction: CO was totally converted to CO_2 but a noticeable amount of hydrogen was also simul-

* Corresponding author. Tel.: +36-1-392-2222/3172; fax: +36-1-392-2533.
E-mail address: wootsch@alpha0.iki.kfki.hu (A. Wootsch).

0021-9517/$ – see front matter
doi:10.1016/j.jcat.2004.04.017

taneously consumed in the presence of excess oxygen. An "optimum" reaction temperature was 100 °C for Rh and Ru [10,11] and around 170 °C for Pt [10,12]. $Co/Cu/Al_2O_3$ and $Ni/Cu/Al_2O_3$ were active in the reaction only above 250 °C, with a 40–50% selectivity at $\lambda = 2$.

Several catalytic systems have been tentatively tested in the PROX reaction so far. The most extensively studied metal is still platinum [12–21], but gold was also found to be a suitable catalyst for the reaction [22–27]. Certain studies deal with the comparison of these two metals [28,29]. Gold catalysts are usually less active but more selective than the Pt ones. Unfortunately, gold also deactivates more rapidly upon long-term operation [25,29].

Other formulations were also tested such as Pt–Sn alloy [30], Ru catalysts [31,32], and Pt, Ru, and Rh containing γ-Al_2O_3–SiO_2 microporous membranes [33]. Ruthenium was found to be superior to platinum. It was active at a lower temperature and resulted in higher selectivities toward CO_2 formation. Nevertheless, methane formation was observed above 250 °C over Ru/Al_2O_3 and hydrogen was again consumed [31].

The usual reactor setup, at a laboratory scale, is a flow reactor operated at atmospheric pressure [10–33]. A two-stage reactor was also reported where oxygen was added to the reaction mixture before and in between the two stages [14]. Half-industrial PROX reactors were developed using Pt–Ru bimetallic catalysts [8,9]. In these cases the chemical process was not described in detail, but considered as mainly oxidation accompanied by methanation and a water–gas-shift reaction.

Existing PROX catalysts might lower the CO concentration in a hydrogen-rich stream under restricted reaction conditions [8,9]. In fact, some problems hamper their application:

(i) The "operating window" is too narrow. Platinum catalysts can be used efficiently in a small temperature range (170–200 °C) and in the presence of excess oxygen, $\lambda = 2.2$ [12].
(ii) The selectivity toward CO oxidation must be increased to minimize the hydrogen lost.
(iii) The effect of the fluctuations in the inlet gas concentration must be compensated.

In our understanding, the CO *oxidation in reductive atmosphere* could be analogous to three-way catalysis (TWC) in the case of automotive exhaust posttreatment. In that case cerium–zirconium mixed oxides are added to the support to promote the oxidation reactions under oxygen-poor conditions [34–36]. Ceria supported platinum [37,38], rhodium [39,40] as well as palladium [41] catalysts are also remarkably active in the low-temperature oxidation of CO. Ceria–zirconia-supported noble metal catalysts, prepared and characterized in our laboratory, were able to oxidize carbon monoxide even in the absence of oxygen [42,43].

Herein we report preferential CO oxidation in the presence of excess hydrogen over $Pt/Ce_xZr_{x-1}O_2$ ($x = 0$, 0.15, 0.5, 0.68, 1) catalysts in comparison with results observed on Pt/Al_2O_3. Our goal was to study the effect of the reaction conditions (T, excess O_2, λ), to compare the different catalysts and to get information on the reaction mechanism.

2. Methods

2.1. Catalysts

An overview of the catalysts is presented in Table 1. Pt/Al_2O_3 was prepared by impregnation of H_2PtCl_6 on a γ-Al_2O_3 support (GFS, BET = 210 m^2/g, precalcined at

Table 1
Characteristics of the Pt catalysts tested in the PROX reaction

	Catalyst	y (%)[a]	D (%)[b]	m (mg)[c]	BET[d] ($m^2\ g^{-1}$)	Cl content[e] (%)	Cl/Pt	(atom/nm^2)
Prepared from H_2PtCl_6	Pt/Al_2O_3	0.6	75	112	207	0.02	0.2	0.02
Prepared from $Pt(NH_3)_4(OH)_2$	Pt/ZrO_2	1	34	102	12	0	–	–
Cl-free ceria-containing	Pt/CeO_2	1	53	100	28	0	–	–
samples, prepared from	$Pt/Ce_{0.68}Zr_{0.32}O_2$	1	67	128	41	0	–	–
$Pt(NH_3)_4(OH)_2$	$Pt/Ce_{0.50}Zr_{0.50}O_2$	1	50	103	40	0	–	–
	$Pt/Ce_{0.15}Zr_{0.85}O_2$	1	48	116	33	0	–	–
Impregnation of Cl ions	Pt/CeO_2 (Cl/Pt = 1)[f]	1	52	112	28	0.15	0.8	0.9
	Pt/CeO_2 (Cl/Pt = 2)[f]	1	53	103	27	0.29	1.6	1.8
	Pt/CeO_2 (Cl/Pt = 4)[f]	1	51	98	28	0.56	3.1	3.4
Prepared from H_2PtCl_6	Pt/CeO_2	1	54	117	26	0.66	3.6	4.3

[a] y, metal content of the catalyst, m/m%.
[b] D, metal dispersion of the catalyst.
[c] m, mass of catalyst placed in the reactor.
[d] Measured after impregnation.
[e] Cl content was measured by elemental analysis (Service Central d'Analyses du CNRS, France). The value in atom/nm^2 is calculated from Cl content (m/m%) and BET surface area.
[f] Cl-free Pt/CeO_2 sample was impregnated by Cl ions in amounts corresponding nominally to 1, 2, and 4 Pt-atom eq.

450 °C, $D_{AIR} = 30$ mL/min). The impregnated sample was washed by bidistilled water, dried overnight at 120 °C, calcined at 300 °C for 4 h in flowing air ($D_{AIR} = 30$ mL/min), and finally reduced at 500 °C for 4 h in flowing H_2 ($D_{H_2} = 30$ mL/min). Dispersion was determined by chemisorption of H_2 at room temperature.

The preparation and the characterization of the ceria–zirconia supports and the corresponding catalysts have already been described elsewhere [34,42–44]. Briefly, the supports (Rhodia Catalysts & Electronics) were precalcined at 900 °C for 6 h ($D_{AIR} = 30$ mL/min) and impregnated using a Cl-free metal salt, $Pt(NH_3)_4(OH)_2$. The received samples were dried at 120 °C for 24 h and calcined for 4 h at 500 °C in flowing air ($D_{AIR} = 30$ mL/min) and reduced at 400 °C for 4 h in flowing H_2 ($D_{H_2} = 30$ mL/min). Finally, the samples were characterized by XRD, TEM, BET, and elemental analysis as well as low temperature (−85 °C) H_2 adsorption [45] to determine the metal dispersion [42–44].

In order to study the effect of Cl ions on the performance of Pt/CeO_2 catalysts in the PROX reaction, a Pt-on-ceria catalyst has been prepared from H_2PtCl_6 and pretreated as above. Other Cl-containing samples were prepared by impregnation of the Cl-free Pt/CeO_2 catalyst by chloride ions, using HCl. Charges of 1 g of this catalyst were immersed in solutions of 0.1 M HCl. The Cl content of the solutions was set at 1, 2, and 4 Pt-atom eq. After evaporation of the solution, the cake was dried at 120 °C overnight and calcined at 400 °C in flowing air for 4 h ($D_{AIR} = 30$ mL/min) and reduced at 400 °C for 4 h in flowing H_2 ($D_{H_2} = 30$ mL/min). The efficiency of chlorination was between 60 and 80% (Table 1). Obviously, some of the Cl left the surface during the pretreating procedure. The chlorination did not really affect the BET surface of the samples (Table 1).

2.2. Reactor setup

Catalytic tests were carried out in an atmospheric continuous flow reactor system. Tubing and connections were made from stainless steel. Analytical grade (Alphagas-1) cylinders of hydrogen, helium, and CO/He 1/1 as well as O_2/He 1/1 mixtures were used as inlet gases and controlled by Brooks mass-flow controllers previously calibrated. Product analysis was preformed by two gas chromatographs:

(i) one equipped with a polar column, Poropak Q, to separate CO_2 and H_2O from the other outlet gases, and
(ii) the other equipped with a 5 Å molecular sieve filled column, for CO and O_2 separation.

In both cases TCD detectors were used. Helium was used as carrier gas for the GCs. Principally, CO_2 and H_2O were detected as the only products. Methane formation did not appear in our experimental conditions. The total gas inlet was 100 N mL/min, containing 70% H_2, 5% CO, 2–5% O_2 (oxygen excess, λ, from 0.8 to 2), and 17–20% He as a balance.

2.3. Calculations

Two competing reactions were taken into consideration: the CO oxidation ($2CO + O_2 \rightarrow 2CO_2$) and the hydrogen oxidation ($2H_2 + O_2 \rightarrow 2H_2O$). The inlet amount of the different gasses is known: $n^{in}_{H_2}$, n^{in}_{CO}, $n^{in}_{O_2}$, n^{in}_{He}. The following equations can be established from the stoichiometry and mass balances:

H,

$$n^{in}_{H_2} = n^{out}_{H_2} + n^{out}_{H_2O}, \tag{1}$$

C,

$$n^{in}_{CO} = n^{out}_{CO} + n^{out}_{CO_2}, \tag{2}$$

O,

$$2 \cdot n^{in}_{O_2} + n^{in}_{CO} = 2 \cdot n^{out}_{O_2} + 2 \cdot n^{out}_{CO_2} + n^{out}_{CO} + n^{out}_{H_2O}, \tag{3}$$

He,

$$n^{in}_{He} = n^{out}_{He}. \tag{4}$$

There are 6 different outlet flows $n^{out}_{H_2}$, n^{out}_{CO}, $n^{out}_{O_2}$, n^{out}_{He}, $n^{out}_{H_2O}$, and $n^{out}_{CO_2}$, respectively. Because of the 4 linearly independent equations (1)–(4), measurement of 2 linearly independent outlet flow rates could define all the outlet parameters. In practice, we determined the outlet amount of CO and O_2 and we used the CO_2 concentration to check the mass balance. Analysis of hydrogen and water only gave approximate values so that the above-noted equations were used to determine their exact concentrations.

The *total conversion* was defined as the oxygen consumption

$$X_{total} = X_{O_2} = \frac{n^{in}_{O_2} - n^{out}_{O_2}}{n^{in}_{O_2}} \cdot 100 \text{ (in \%)}. \tag{5}$$

The *selectivity* was calculated as the ratio of the desired reaction (CO oxidation) to the overall reactions, H_2 and CO consumption. Such a definition of the selectivity is also valid when methane formation occurs

$$S = \frac{\Delta CO}{\Delta CO + \Delta H_2} \cdot 100 = \frac{n^{in}_{CO} - n^{out}_{CO}}{n^{in}_{CO} - n^{out}_{CO} + n^{in}_{H_2} - n^{out}_{H_2}} \cdot 100 \text{ (in \%)}. \tag{6}$$

The *selectivity* can also be defined as the ratio of the oxygen transformed into CO_2 to the total oxygen consumed. When no methane is formed: Eq. (6) = Eq. (7). Thus, from Eqs. (1)–(3) and (6):

$$S = \frac{n^{out}_{CO_2}}{2 \cdot (n^{in}_{O_2} - n^{out}_{O_2})} \cdot 100 \text{ (in \%)}. \tag{7}$$

The *CO conversion*, in fact, can be defined as

$$X_{CO} = \frac{n^{in}_{CO} - n^{out}_{CO}}{n^{in}_{CO}} \cdot 100 = \frac{n^{out}_{CO_2}}{n^{in}_{CO}} \cdot 100 \text{ (in \%)}. \tag{8}$$

Lambda (λ) is the oxygen excess factor. By definition

$$\lambda = \frac{2 \cdot n_{O_2}^{in}}{n_{CO}^{in}} = \frac{2 \cdot p_{O_2}}{p_{CO}} = \frac{2 \cdot [O_2]^{in}}{[CO]^{in}} = \frac{2 \cdot c_{O_2}^{in}}{c_{CO}^{out}}. \quad (9)$$

$\lambda = 1$ means that oxygen is present in stoichiometric amount, $\lambda > 1$ corresponds to an oxygen excess compared to pure CO oxidation, and $\lambda < 1$ corresponds to a deficit in oxygen compared to pure CO oxidation.

It must be noted that the product of the total conversion (X_{O_2}) with the selectivity (S) does not directly result in the CO conversion. The oxygen excess must be taken into account. Then, from Eqs. (5), (7)–(9):

$$X_{CO} = \frac{S \cdot X_{O_2}}{100} \cdot \lambda \text{ (in \%)}. \quad (10)$$

3. Results

Fig. 1 presents the results obtained over Pt/Al_2O_3. These results corresponded well to typical literature values [10,12,16]. The oxygen conversion increased slightly but significantly with increasing λ, probably due to the positive oxygen order earlier observed for Pt catalysts [12]. Nevertheless, platinum showed a *natural selectivity* toward CO oxidation as lower λ values resulted in higher selectivity. The selectivity showed a maximum as a function of temperature at all λ values (Fig. 1).

Platinum on ceria catalysts showed a different behavior (Fig. 2). The oxygen conversion was very high, even at low temperatures. We observed a sharp "light off" around 90 °C (Fig. 2), according to the observations in the CO oxidation reaction [37–39]. The maximum in the selectivity as a function of temperature was observed at a much lower temperature than on Pt/Al_2O_3 or did not even appear (cf. Figs. 1

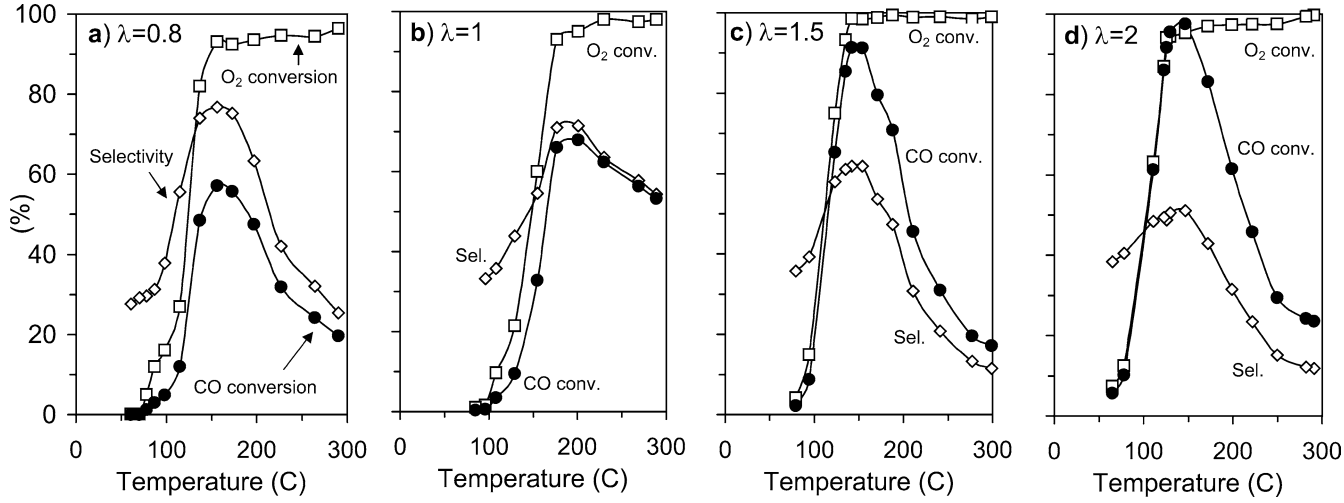

Fig. 1. Preferential oxidation of CO on the Pt/Al_2O_3 catalyst. Oxygen conversion (□), selectivity toward CO oxidation (◇), and CO conversion (●) as a function of temperature at different oxygen excess, (a) $\lambda = 0.8$, (b) $\lambda = 1$, (c) $\lambda = 1.5$, (d) $\lambda = 2$.

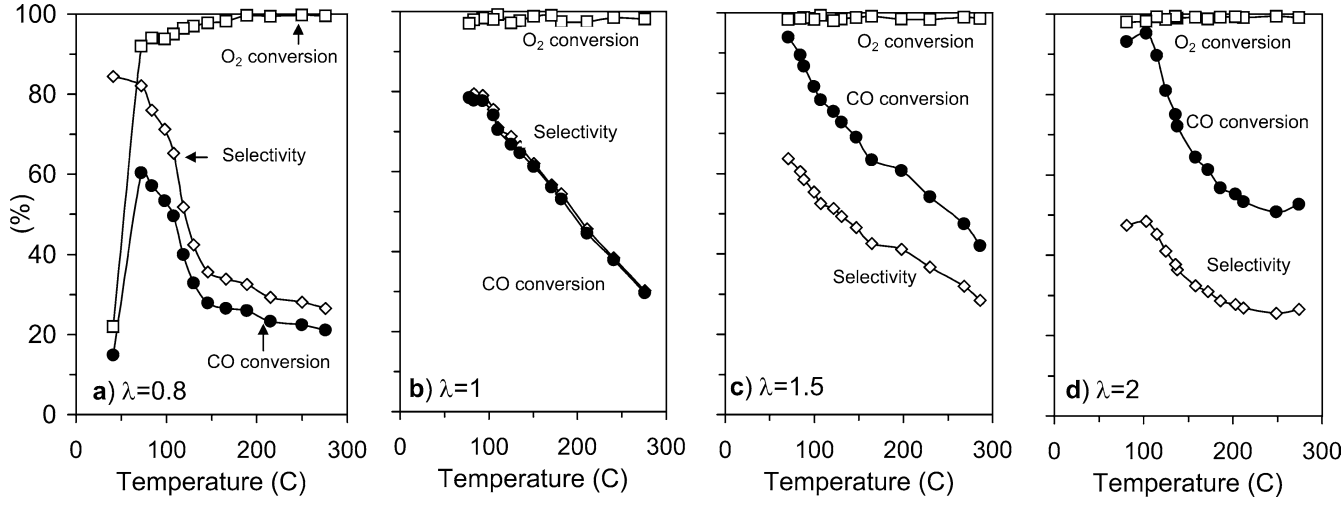

Fig. 2. Preferential oxidation of CO on the Cl-free Pt/CeO_2 catalyst. Oxygen conversion (□), selectivity toward CO oxidation (◇), and CO conversion (●) as a function of temperature at different oxygen excess, (a) $\lambda = 0.8$, (b) $\lambda = 1$, (c) $\lambda = 1.5$, (d) $\lambda = 2$.

Table 2
PROX reaction on the different Pt catalysts at selected temperatures at $\lambda = 1$ and $\lambda = 2$ X_{CO}, CO conversion; X_{O_2}, oxygen conversion; S, selectivity toward CO oxidation

Catalyst	$\lambda = 1$			$\lambda = 2$		
	X_{CO} (%)	X_{O_2} (%)	S (%)	X_{CO} (%)	X_{O_2} (%)	S (%)
(a) $T = 100\,^{\circ}C$						
Pt/Al_2O_3	0.7	1.6	43	10	12	40
Pt/CeO_2 (Cl-free)	78	98	80	95	98	48
$Pt/Ce_{0.68}Zr_{0.32}O_2$	74	93	79	59	98	30
$Pt/Ce_{0.50}Zr_{0.50}O_2$	69	99	70	76	97	39
$Pt/Ce_{0.15}Zr_{0.85}O_2$	57	98	58	60	99	30
Pt/ZrO_2	58	95	60	98	98	50
(b) $T = 150\,^{\circ}C$						
Pt/Al_2O_3	33	60	55	98	95	51
Pt/CeO_2 (Cl-free)	61	99	62	65	99	33
$Pt/Ce_{0.68}Zr_{0.32}O_2$	55	93	59	34	97	18
$Pt/Ce_{0.50}Zr_{0.50}O_2$	44	99	45	53	98	27
$Pt/Ce_{0.15}Zr_{0.85}O_2$	38	98	39	36	99	18
Pt/ZrO_2	29	97	30	88	98	45
(c) $T = 200\,^{\circ}C$						
Pt/Al_2O_3	68	98	71	61	97	32
Pt/CeO_2 (Cl-free)	44	97	45	55	99	28
$Pt/Ce_{0.68}Zr_{0.32}O_2$	43	94	46	32	96	17
$Pt/Ce_{0.50}Zr_{0.50}O_2$	33	98	34	37	97	19
$Pt/Ce_{0.15}Zr_{0.85}O_2$	31	99	31	34	98	17
Pt/ZrO_2	23	98	24	75	98	38

and 2). Accordingly this catalyst adequately converted CO at temperatures around 100 °C.

Different cerium–zirconium mixed oxides as well as zirconia-supported Pt catalysts have also been examined in the PROX reaction (Table 2). It must be considered that zirconia is not an active support for the oxygen storage as opposed to ceria or cerium–zirconium mixed oxides [36]. However, ZrO_2 has a better oxygen mobility than alumina, even if it is much less than CeO_2–ZrO_2 [46]. Moreover, some oxygen vacancies could exist on zirconia at the periphery of Pt particles. Consequently, the behavior of ZrO_2 should be intermediary between that of alumina and those of $Ce_xZr_{x-1}O_2$ ($x \neq 0$) supports (Table 2). Pt on $Ce_xZr_{x-1}O_2$ catalysts showed the same kind of behavior as Pt/CeO_2. Table 2 illustrates that the oxygen conversion over these catalysts, active in the oxygen storage, was always around 100%. These catalysts could convert remarkable amount of carbon monoxide at low temperature, even at low oxygen excess (Table 2). At higher temperature, however, they were *too active* to be able to selectively oxidize CO. In this range Pt/Al_2O_3 resulted in higher selectivity toward CO oxidation. Both Pt/Al_2O_3 and Pt/ZrO_2 catalysts showed a maximum selectivity as a function of temperature, but this optimum appeared at lower temperature in the case of the ZrO_2 support.

The presence of chloride ions dramatically decreases the oxygen spillover and back-spillover rates by forming CeOCl species on the ceria support [47]. Such CeOCl species formation decreases the number of available hydroxyl groups, which were claimed to be one key parameter responsible for the possible migration of chemisorbed oxygen species [39,48]. Fig. 3 shows the performance of a Pt–ceria system in the PROX reaction as a function of Cl content on the samples. Oxygen conversion was hardly affected by the presence of Cl (Fig. 3). The selectivity toward carbon dioxide formation, in turn, diminished over chlorinated samples. The effect of chloride ions, as a rule, was more important at low temperatures and at low oxygen excess (Fig. 3). The CO conversion sharply decreased in the case of the catalyst prepared from H_2PtCl_6 precursor (Fig. 3). Obviously, the Cl concentration in the vicinity of Pt particles is higher when a Cl-containing precursor is used, while random Cl deposition on the support can be suggested when chlorine is impregnated on the catalyst afterward. These results also point to the important role of oxygen mobility that will be discussed in detail in the next section.

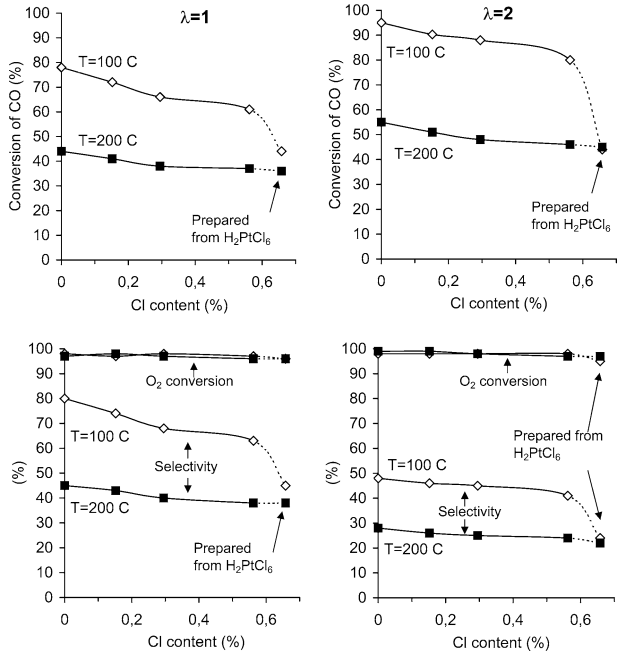

Fig. 3. Effect of chlorine on the catalytic performances of 1% Pt/CeO_2 catalysts in the PROX reaction at 100 °C (◇) and 200 °C (■), at oxygen excess $\lambda = 1$ (left) and $\lambda = 2$ (right). The Pt/CeO_2 catalyst at 0 point was prepared from $Pt(NH_3)_4(OH)_2$ precursor; this sample was impregnated by chloride ions, using HCl in amounts corresponding nominally to 1, 2, and 4 Pt-atom eq. Results are also shown on a Pt/CeO_2 sample prepared from H_2PtCl_6 precursor. The x axis represents the measured Cl content of the catalysts (Table 1).

4. Discussion

4.1. Mechanistic consideration

The overall picture is different, as a rule, on the supports that are active or inactive in the oxygen storage. It might derive from a different reaction mechanism.

The maximum selectivity toward CO oxidation that appeared as a function of temperature in the case of Pt/Al_2O_3 catalyst (Fig. 1) has been explained by competitive Langmuir–Hinshelwood kinetics [12,16,28]: Pt adsorbs all reactants and oxygen alternatively reacts with H_2 or CO. The selectivity toward CO oxidation would thus depend only on the ratio of θ_{CO} to θ_{H_2}. We recall that the heat of CO adsorption on Pt is about 17 kJ/mol higher than the value for hydrogen [49]. As a consequence the θ_{CO}:θ_{H_2} ratio decreases with increasing temperature and the selectivity toward CO oxidation as a function of temperature should continuously decrease. The CO coverage is reported to be close to saturation in the low temperature range (90–180 °C) [12,28]. Calculation upon DRIFT results showed that for a CO partial pressure of 10 kPa, θ_{CO} is higher than $0.9\theta_{saturation}$ up to 200 °C [28]. At the same time the catalytic activity in the CO oxidation of Pt/Al_2O_3 is poor at low temperature ($T < 150$ °C) both in the absence [12] and in the presence of H_2 (Fig. 1). Hydrogen oxidation, in turn, is instantaneous even at room temperature over Pt/Al_2O_3 [50]. Thus, at low temperature, with poor catalytic activity, hydrogen oxidation is preferred, even though θ_{H_2} is very small (compared to θ_{CO} [16]). At this temperature, the rate constant is the limiting factor and it is obviously higher for H_2 [50]. Increasing the temperature leads to an increase in the total catalytic activity and since θ_{CO}:θ_{H_2} is high; the selectivity toward CO oxidation increases (Fig. 1). On the contrary, at a higher temperature ($T > 190$ °C) O_2 conversion is total and accessible oxygen becomes rate limiting [12]. The CO coverage is not any more close to saturation [16] and so θ_{CO}:θ_{H_2} decreases remarkably. From this point hydrogen and CO compete for oxygen. Their coverage ratio governs the selectivity that should decrease.

In the case of ceria and ceria–zirconia-supported samples, no maximum was found (Fig. 2). Since the active phase is platinum in all cases, one might expect to use the same competitive Langmuir–Hinshelwood kinetics to describe these systems too. On the other hand, ceria and cerium–zirconium mixed oxides are reducible supports, active in oxygen storage [34–46], and a noncompetitive Langmuir–Hinshelwood mechanism can be imagined on the metal/oxide interface. It means reaction between CO adsorbed on Pt particles and oxygen activated on the support. Such a noncompetitive mechanism was proposed for the PROX reaction on Fe-promoted Pt/Al_2O_3 [18], bimetallic PtSn catalysts [30], and Au/Fe_2O_3 [23]. The heat of adsorption of the different molecules on Pt particles is, indeed, hardly affected by the presence of ceria support [51,52]. On the contrary, at the metal–ceria interface the kinetics for oxygen spillover may play a role that is more important than the heat of adsorption measured under equilibrium conditions. Accordingly, the participation of surface oxygen from the support during the low-temperature CO oxidation on ceria-supported noble metal catalysts has already been proved both:

(i) from observation of zero-order oxygen pressure dependence [41], and
(ii) by oxygen-exchange measurements between $C^{16}O$ and ^{18}O-predosed catalysts [39].

The results observed on Cl-containing samples also support the idea of a noncompetitive mechanism at the metal/support interface. The presence of chloride ions in the vicinity of Pt particles remarkably reduces the oxygen spillover activity [39,47,48]. Accordingly, the CO-oxidation activity decreased with increasing the Cl content, particularly at low temperature and lower λ values, where oxygen mobility can be the important factor (Fig. 3). However, oxygen conversion remained the same, indicating that the oxygen excess was used up for the hydrogen oxidation. Accordingly, the occurrence of H_2 oxidation does not need oxygen coming from the support, because H is less strongly adsorbed than O on platinum [51,52]. It is not the case for CO. In fact, θ_{CO} is close to saturation at low temperature [28], where the effect of Cl was more pronounced. So, an oxygen flux coming from the support can effectively promote the CO oxidation in this temperature range. This phenomenon leads to two possible conclusions:

(i) CO oxidation preferentially occurs at the metal/support interface, and
(ii) hydrogen may be preferentially oxidized by separate routes, on metal particles or probably on the support alone.

In fact, ceria and CeO_2–ZrO_2 mixed oxides can adsorb hydrogen even in the absence of noble metal particles [53]. Hydrogen can then desorb both in the form of H_2 (reversible adsorption) and H_2O (irreversible adsorption) [53]. This later process means, indeed, hydrogen oxidation on the support. Such reaction was observed above 130 °C [53].

Platinum is claimed to be an active catalyst in the water–gas-shift reaction above 200 °C. Pt-on-ceria showed particularly high activity [54]. The effect of water has been studied indirectly: increasing O_2 excess results in an increasing amount of water in the reactor because the excess oxygen reacts with hydrogen (Figs. 1 and 2). This water, formed by H_2 oxidation, can react with CO in a WGS reaction. This process would virtually result in higher selectivity toward CO_2 formation. Accordingly, at $\lambda = 2$ and above 200 °C, we observed that the selectivity toward CO oxidation on the Pt/CeO_2 sample is about constant or slightly increasing with temperature, while it decreases at lower λ values (Fig. 2).

In summary, all processes are possible, i.e.,

(i) competitive Langmuir–Hinshelwood CO and hydrogen oxidation on Pt particles, mostly in the case of Pt/Al_2O_3,
(ii) noncompetitive Langmuir–Hinshelwood mechanism on the metal/oxide interface, in the case of reducible support,

(iii) hydrogen direct oxidation on the ceria(–zirconia) support, and
(iv) water–gas-shift reaction at high temperature, particularly on ceria-containing samples.

The second reaction route is predominant on Pt-on-ceria–zirconia samples at low temperatures (90–130 °C) and CO is preferentially oxidized rather than hydrogen. This process was selectively blocked by Cl ions. At higher temperatures, H_2 oxidation on the ceria support may also be an important process. The coexistence of these mechanisms

(i) can be the reason for the high activity of ceria-supported catalysts, and
(ii) can explain the continuous increase in the selectivity with decreasing temperature.

4.2. Optimum catalytic formulation

One of the critical questions is: "What is the best PROX catalyst?" Of course an *ideal* PROX catalyst

(i) would be 100% selective toward CO oxidation when $\lambda \leqslant 1$, and
(ii) would convert all CO when $\lambda \geqslant 1$.

We suggest that an effective comparison between the different catalysts can easily be done in a visualization such as Fig. 4. The ideal PROX catalyst would result in a vertical line at $x = 0$ (y axis), meaning 0% hydrogen loss, and then in a horizontal line at 100% CO conversion. This later case is possible only when $\lambda \geqslant 1$.

Fig. 4 shows the conversion of CO as a function of the hydrogen loss for Pt/Al_2O_3 (Fig. 4a) and for the Cl-free Pt/CeO_2 (Fig. 4b). Data obtained at the same oxygen excess are connected forming a line at "iso-lambda." The highest CO conversion values at a given H_2 loss are linked by a thick line (Fig. 4). Points above this line cannot be reached under the selected reaction conditions; so we called this area the "prohibited region." We believe that the iso-lambda curves, observed under the same conditions on different catalysts, can serve for comparison purposes. The prohibited region was somehow smaller in the case of ceria-supported Pt catalyst than on Pt/Al_2O_3 (Fig. 4).

It must be noted that the extent of the prohibited region also depends on the reaction conditions, and not only on the catalyst nature. We used 5% CO in the inlet stream. Obviously, lower inlet CO concentration would result in a curve being closer to the y axis, since (at a constant λ value) lower amounts of O_2 would be added to the reaction mixture, resulting in lower loss in H_2. On the other hand, the absolute value of CO determines the surface coverage of the catalyst [12,28]. If the CO concentration decreased to a value when θ_{CO} is not close to saturation any more, selectivity toward CO oxidation would decrease. Other operating parameters, in turn, hardly affect the area of the prohibited region.

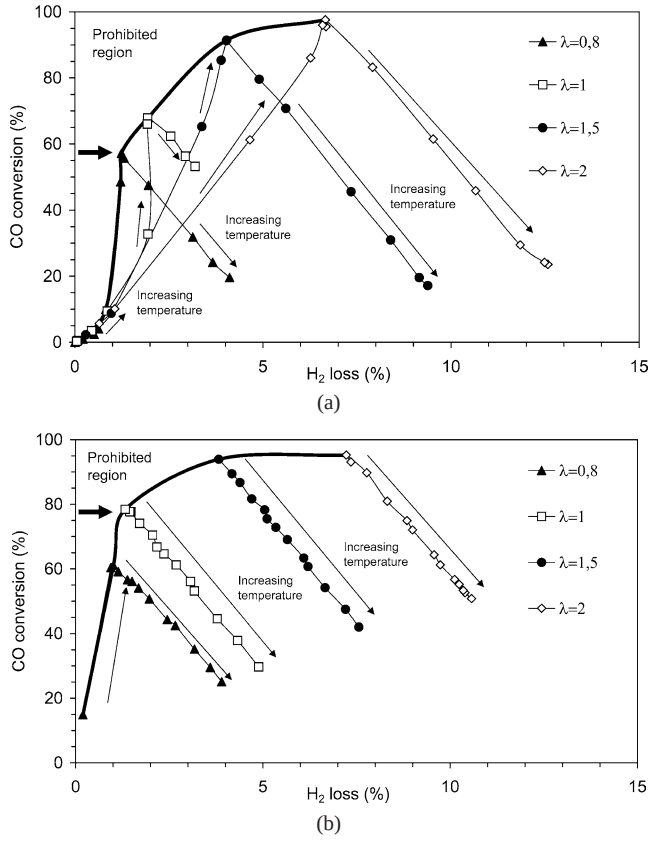

Fig. 4. Conversion of carbon monoxide as a function of the hydrogen loss (H_2 conversion) on Pt/Al_2O_3 (a) and on the Cl-free Pt/CeO_2 catalyst (b). Data in (a) correspond to Fig. 1 and in (b) to Fig. 2. The reaction temperature increased in the direction of the thin arrows. Results above the thick line, "prohibited region," cannot be reached under any reaction conditions. Thick arrows: optimal operating point in a multistage reactor system; see text.

In fact, the maximum CO conversion (selectivity) is rather contact time independent in a wide range [12,16]. The conditions we used (100 mL/min total flow, 100 mg catalyst) were in this range, corresponding well to that commonly reported in the literature [12,14,16,22,25,28,29,33]. Furthermore, using more catalyst would not lead to higher CO conversion since the oxygen conversion is total at maximum CO conversion (Figs. 1 and 2). The selectivity increased monotonously with decreasing temperature on Pt/ceria (Fig. 2). However, the CO conversion cannot be further increased by decreasing the temperature because of the sharp light off observed in this case (Fig. 2). As a conclusion, a visualization such as Fig. 4 is characteristic for a PROX catalyst at a given CO inlet concentration (5% in our case).

On Pt/Al_2O_3 a maximum in selectivity is observed as a function of temperature (Fig. 1). Such maxima are also visible in Fig. 4a. On the other hand, in the case of Pt/CeO_2 catalyst, straight iso-lambda lines were formed (Fig. 4b). In both cases any selected CO conversion can be reached at various λ values and different temperatures. However, it is obvious that one should work close to the thick line, at low hydrogen loss. Nevertheless, this line converges to 100% CO conversion but does not reach it under the examined experimental

conditions. By extrapolating the line one may estimate that a minimum 10% hydrogen would be lost at 99% CO conversion. This problem can be solved by applying a multistage reactor adding extra oxygen in between the two stages [14]. For example, two subsequent PROX reactors, both working at 90% CO conversion, would result in about 99% CO conversion at a much lower hydrogen loss. For minimizing the hydrogen loss, one must use consecutive reactors operated at a point just before the H_2 loss increases sharply while CO conversion levels up (thick arrows in Fig. 4). In the case of ceria-supported Pt this point is around $\sim 80\%$ CO conversion at $\lambda \approx 1$, while in the case of Pt on Al_2O_3 it is around 60% CO conversion at $\lambda \approx 0.8$. Fig. 4, thus, clearly shows the optimal operating point at a given inlet CO concentration (thick arrows). The CO conversion is not sufficient here, but it can be improved in a second reactor stage. The efficiency of the overall process, in turn, is the highest at this point.

Ceria can be an adequate support for Pt when one has to lower the CO concentration in a hydrogen-rich stream by using the PROX reaction at low temperature and/or with a minimum hydrogen loss. Unfortunately, ceria-supported platinum was found to be *too active* in hydrogen oxidation as well, and cannot be considered as an effective PROX catalyst above 130 °C. Nevertheless, ceria can be considered as a beneficial additive to supported Pt catalysts [21]. Pt/CeO_2-(–ZrO_2) catalysts could also be introduced as an effective part in a multistage PROX reactor system.

Acknowledgments

Most of the present work was carried out during the postdoctoral fellowship of Attila Wootsch in Poitiers, sponsored by both the French Ministry of Foreign Affairs (from 1 October 2001 to 31 December 2001) and by the Région Poitou-Charentes (from 15 January 2002 to 15 November 2002). Additional mutual visits were part of the cooperation between the Hungarian Academy of Sciences and the CNRS. These financial supports are gratefully acknowledged. Thanks to Dr. Sumeya Bedrane, Dr. Christelle Carnevillier, and Ms. Mélanie Pajon for their help in catalyst preparation.

References

[1] A.J. Appleby, F.R. Foulkes, Fuel Cell Handbook, Van Nostrand Reinhold, New York, 1989.
[2] W. Vielstich, T. Iwasita, in: G. Ertl, H. Knözinger, J. Weitkamp (Eds.), Handbook of Heterogeneous Catalysis, vol. 4, Verlag Chemie, Weinheim, 1997, p. 2090.
[3] R.A. Lemons, J. Power Sources 29 (1990) 251.
[4] J.M. Zalc, D.G. Löffler, J. Power Sources 111 (2002) 58.
[5] J.N. Armor, Appl. Catal. 176 (1999) 159.
[6] F. Joensen, J.R. Rostrup-Nielsen, J. Power Sources 105 (2002) 195.
[7] F. Auprêtre, C. Descorme, D. Duprez, Catal. Commun. 3 (2002) 263.
[8] C.D. Dudfield, R. Chen, P.L. Adcock, Int. J. Hydrogen Energy 26 (2001) 763.
[9] S.H. Lee, J. Han, K.-Y. Lee, J. Power Sources 109 (2002) 394.
[10] S.H. Oh, R.M. Sinkevitch, J. Catal. 142 (1993) 254.
[11] Y.-F. Han, M.J. Kahlich, M. Kinne, R.J. Behm, PCCP 4 (2002) 389.
[12] M.J. Kahlich, H.A. Gasteiger, R.J. Behm, J. Catal. 171 (1997) 93.
[13] O. Korotkikh, R. Farrauto, Catal. Today 62 (2002) 249.
[14] H. Igarashi, H. Uchida, M. Suzuki, Y. Sasaki, M. Watanabe, Appl. Catal. 159 (1997) 159.
[15] M.M. Schubert, A. Gasteiger, R.J. Behm, J. Catal. 172 (1997) 256.
[16] H.D. Kim, M.S. Lim, Appl. Catal. A 224 (2002) 27.
[17] A. Manaslip, E. Gulari, Appl. Catal. B 37 (2002) 17.
[18] X. Liu, O. Korotkikh, R. Farrauto, Appl. Catal. A 226 (2002) 293.
[19] I.H. Son, M. Shamsuzzoha, A.M. Lane, J. Catal. 210 (2002) 460.
[20] I.H. Son, A.M. Lane, Catal. Lett. 76 (2001) 151.
[21] S. Özkara, A.E. Aksoylu, Appl. Catal. A 251 (2003) 75.
[22] G.K. Bethke, H.H. Kung, Appl. Catal. 194–195 (2000) 43.
[23] M.J. Kahlich, H. Gasteiger, R.J. Behm, J. Catal. 182 (1999) 430.
[24] R.J.H. Grisel, B.E. Nieuwenhuys, J. Catal. 199 (2001) 48.
[25] M.M. Schubert, V. Plzak, J. Garche, R.J. Behm, Catal. Lett. 76 (2001) 143.
[26] B. Rohland, V. Plzak, J. Power Sources 84 (1999) 183.
[27] H.-S. Oh, J.H. Yang, C.K. Costello, Y.M. Wang, S.R. Bare, H.H. Kung, M.C. Kung, J. Catal. 210 (2002) 375.
[28] M.M. Schubert, M.J. Kahlich, H.A. Gasteiger, R.J. Behm, J. Power Sources 84 (1999) 175.
[29] G. Avgouropoulos, T. Ioannides, Ch. Papadopoulou, J. Batista, S. Hocevar, H.K. Matralis, Catal. Today 75 (2002) 157.
[30] M.M. Schubert, M.J. Kahlich, G. Feldmeyer, M. Hüttner, H.A. Hackenberg, H.A. Gasteiger, R.J. Behm, PCCP 3 (2001) 1123.
[31] Y.-F. Han, M.J. Kahlich, M. Kinne, R.J. Behm, PCCP 4 (2002) 389.
[32] A. Wörner, C. Friedrich, R. Tamme, Appl. Catal. A 245 (2003) 1.
[33] Y. Hasegawa, A. Ueda, K. Kusakabe, S. Morooka, Appl. Catal. A 225 (2002) 109.
[34] Y. Madier, C. Descorme, A.M. Le Govic, D. Duprez, J. Phys. Chem. B 103 (1999) 10999.
[35] A. Trovarelli, Catal. Rev.-Sci. Eng. 38 (1996) 439.
[36] A. Galdikas, C. Descorme, D. Duprez, Solid State Ionics 166 (2004) 147.
[37] Y.Y. Yung-Fang, J. Catal. 87 (1984) 152.
[38] S. Johansson, L. Österlund, B. Kasemo, J. Catal. 201 (2001) 275.
[39] R. Taha, D. Martin, S. Kacimi, D. Duprez, Catal. Today 29 (1996) 89.
[40] T. Bunluesin, H. Cordatos, R.J. Gorte, J. Catal. 157 (1995) 222.
[41] E. Bekyarova, P. Fornasiero, J. Kaŝpar, M. Graziani, Catal. Today 45 (1998) 179.
[42] S. Bedrane, C. Descorme, D. Duprez, Catal. Today 73 (2002) 233.
[43] S. Bedrane, C. Descorme, D. Duprez, Catal. Today 75 (2002) 401.
[44] C. Descorme, Y. Madier, D. Duprez, J. Catal. 196 (2000) 167.
[45] A. Holmgren, B. Andersson, J. Catal. 178 (1998) 14.
[46] D. Martin, D. Duprez, J. Phys. Chem. 101 (1997) 4428.
[47] D.I. Kondarides, X.E. Verykios, J. Catal. 174 (1998) 52.
[48] S. Bernal, J.J. Calvino, G.A. Cifredo, J.M. Rodríguez-Izquierdo, V. Perrichon, A. Laachir, J. Catal. 137 (1992) 1.
[49] B. Sen, M.A. Vannice, J. Catal. 130 (1991) 9.
[50] M.T. Janicke, H. Kestenbaum, U. Hagendorf, F. Schuth, M. Fichtner, K. Schubert, J. Catal. 191 (2000) 282.
[51] G.S. Zafiris, R.J. Gorte, Surf. Sci. 276 (1992) 86.
[52] T. Chafik, O. Dulaurent, J.L. Gass, D. Bianchi, J. Catal. 179 (1998) 503.
[53] S. Bernal, J.J. Calvino, G.A. Cifredo, J.M. Gatica, J.A.P. Omil, J.M. Pintado, J. Chem. Soc., Faraday Trans. 89 (1993) 3499.
[54] J. Barbier Jr., D. Duprez, Appl. Catal. B 3 (1993) 461.